

## Simultaneous Measurements of Gaseous Nitrous Acid and Particulate Nitrite Using Diffusion Scrubber/Steam Chamber/Luminol Chemiluminescence

Wonil Chang,<sup>a</sup> Jungho Choi, Sangbum Hong,<sup>b,\*</sup> and Jai H. Lee

Advanced Environmental Monitoring Research Center (ADERC), Department of Environmental Science and Engineering, Gwangju Institute of Science and Technology (GIST), Gwangju 500-701, Korea. \*E-mail: lighthsb@cheju.ac.kr

Received November 9, 2007

An instrument was developed for the simultaneous determination of gas- and aerosol-phase nitrous acid (HONO). Gaseous HONO (HONO(g)) was sampled by a diffusion scrubber and particulate nitrite (NO<sub>2</sub><sup>-</sup>(p)) was collected by a particle growth chamber. The collected samples were analyzed in time-sharing manner, based on the peroxyxynitrite-induced luminol chemiluminescence. The automated system was found to be sensitive with 13 pptv of detection limit, fast with 4 min. of sampling frequency, and simple and affordable to construct and operate. The system was optimized by adjusting the experimental parameters. The system was applied to the field measurement of gas- and particle-phase HONO during the springtime of 2004 in Gwangju, South Korea. HONO(g) concentrations varied diurnally from 200 pptv around 3 P.M. to 800 pptv at 5 A.M. The variation of NO<sub>2</sub><sup>-</sup>(p) was not significant with the maximum of 240 pptv at 11 P.M. and the minimum of 170 pptv at 4 P.M., not displaying distinct characteristics.

**Key Words :** Gaseous HONO, Particulate nitrite, Instrumentation, Field measurements

### Introduction

Gas-phase nitrous acid (HONO(g)) is an important photochemical constituent due to its close relationship with odd-nitrogen species (*e.g.*, NO<sub>x</sub>) and atmospheric cleansing power, roughly represented by a global average concentration of OH radical.<sup>1</sup> Particularly, in the morning boundary layer, HONO(g) can be a dominant source of OH radical production *via* its photolysis partly due to low concentrations of other major oxidants such as ozone and formaldehyde<sup>2-4</sup> and its absorption of visible radiation in wider range than the other oxidants. Recent studies indicated that HONO(g) photo-dissociation could be responsible, up to 34%, for the total daily OH production in polluted boundary layer.<sup>3,4</sup>

Sources of HONO(g) include homogeneous gas-phase reactions, heterogeneous reactions, and direct emission. Its sinks are photolysis, OH attack, and dry and wet deposition. In particular, heterogeneous reactions of NO<sub>2</sub> on various surfaces are recognized to play a major role in HONO(g) production during nighttime, however detailed chemical mechanisms are not well understood.<sup>2,5,6</sup>

Since the first reliable measurement of HONO(g) was feasible by employing differential optical absorption spectroscopy (DOAS),<sup>7,8</sup> a variety of other techniques have been developed. These methods can be in large classified into two groups, optical analyses and surface collection followed by various chemical analyses.<sup>9,10</sup> The optical methods include DOAS and UV-photofragmentation/laser-induced fluorescence sensor.<sup>11</sup> The surface collection methods encompass

alkaline coated annular denuder/ion chromatography (IC),<sup>12-14</sup> diffusion scrubber/chemiluminescence,<sup>15</sup> diffusion scrubber/IC,<sup>16</sup> stripping coil/Dinitrophenylhydrazine/HPLC,<sup>17</sup> and wet effluent diffusion denuder/IC.<sup>18-21</sup> These methods have their own strengths and weaknesses.<sup>2,17</sup> Some suffer from poor detection limits while others require too long integration time and/or tedious labor. More details can be found in literature.<sup>2,9,22,23</sup>

The application of DOAS method to field studies can be restricted under adverse meteorological conditions such as poor visibility and atmospheric turbulence since it demands long light pathway (about 400-3000 m). This system is neither plain nor easy to construct and operate, and has limited mobility. In addition, it cannot analyze NO<sub>2</sub><sup>-</sup>(p).<sup>7,8</sup> UV-photofragmentation/laser-induced fluorescence sensor has been deterred by the complexity and the sizable instrument cost. It is technically complex, uses corrosive chemicals, and requires large amount of electrical power. As in DOAS, NO<sub>2</sub><sup>-</sup>(p) can not be analyzed by this technique.<sup>11</sup> Alkaline coated annular denuder/ion chromatography provides the advantages of being relatively simple and inexpensive with a portable collection system. However, the detection limit is 400 pptv for 6 hr integration time and thus this method requires long sampling time. It also suffers from some inherent drawbacks such as being labor-intensive and being prone to interference from surface reactions of NO<sub>x</sub> within the apparatus.<sup>12-14</sup> Diffusion scrubber/IC,<sup>16</sup> stripping coil/Dinitrophenylhydrazine/HPLC,<sup>17</sup> wet effluent diffusion denuder/IC<sup>18-21</sup> offer advantages such as relatively high sensitivity, moderately low cost, ease of automation, adaptation to a mobile platform but time resolution are relatively not good due to use of chromatography system.

Although a large number of measurements have been made for HONO(g) and NO<sub>2</sub><sup>-</sup>(p), most experiments were

<sup>a</sup>Present address: Department of Earth and Environmental Sciences, Korea University, Seoul 136-701, Korea

<sup>b</sup>Present address: Research Institute for Basic Sciences and Department of Chemistry, Cheju National University, Jeju 690-756, Korea

conducted for either gas- or aerosol-phase. Only in a handful of studies, both species were concurrently measured.<sup>20,21,24-28</sup>

Li (1994) found that in an arctic area during the polar sunrise period, the ratio of  $\text{NO}_2^-(\text{p})$  to  $\text{HONO}(\text{g})$  was increased from 0.1 to sometimes greater than 1 with time. In a field experiment conducted in Lubbock, Texas, particulate and gaseous HONO were found to be strongly correlated and  $\text{NO}_2^-(\text{p})/\text{HONO}(\text{g})$  ratios were approximately from 0.5 to 0.8.<sup>20</sup> In Central Switzerland, Neftel *et al.* (1996) observed that particle-phase HONO ranged between approximately 5 and 10% of gas-phase HONO. In Zurich, Switzerland, the ratio of  $\text{NO}_2^-(\text{p})$  to total HONO ( $\text{NO}_2^-(\text{p}) + \text{HONO}(\text{g})$ ) was found to vary from 25% to 41%, depending on time of the year.<sup>24</sup> At a rural site in the Amazon Basin, concentrations of  $\text{HONO}(\text{g})$  and  $\text{NO}_2^-(\text{p})$  were substantially higher during the dry season than the wet season.<sup>26</sup> This was attributed to the biomass burning frequently observed during the dry period. Over the same period,  $\text{NO}_2^-(\text{p})$  constituted up to 25% of  $\text{HONO}(\text{g})$  on the basis of the diurnal maxima. All these results suggest that a significant fraction of total HONO can be present as the aerosol-phase, and the ratio of  $\text{NO}_2^-(\text{p})$  to  $\text{HONO}(\text{g})$  shows a wide range of spatial and temporal variations. For more accurate determination of their fractions, therefore, it is necessary to measure both species simultaneously.

Significances of this study are two-fold. First, an instrument for  $\text{HONO}(\text{g})$  measurement was developed to make simultaneous measurements of the gas- and particle-phase HONO. Our system was made up of diffusion scrubber, particle collection system, and luminol chemiluminescence detector to overcome the disadvantages of other instrumentations mentioned above. Secondly, by means of the instrument with low LOD (13 pptv) and 4 min time resolution, results of field observations were presented.

### Experimental Section

In this study, measurements of  $\text{HONO}(\text{g})$  and  $\text{NO}_2^-(\text{p})$  were based on diffusion scrubber/steam reactor/luminol chemiluminescence. As illustrated in Figure 1, this instrument is composed of three main systems: a sampling system, an automated sample injection system, and an analytical system. In the sampling system, DS was used to separately collect  $\text{HONO}(\text{g})$  and  $\text{NO}_2^-(\text{p})$  both of which were transferred to the respective stream channel. In the injection system, the samples were driven alternately into the analytical system through six-port valve (V). Sample loads and injection time durations in the valves were controlled by a time controller. Finally, the analytical system was based on the reaction of peroxyxynitrite with luminol reagent to produce chemiluminescent light, detected by a photomultiplier tube (PMT) to quantify  $\text{HONO}(\text{g})$  and  $\text{NO}_2^-(\text{p})$ .

**Sampling system.** Air samples, containing  $\text{HONO}(\text{g})$  and  $\text{NO}_2^-(\text{p})$  both, were drawn into the sampling system at a flow rate of  $1 \text{ L min}^{-1}$  by a vacuum pump (A), set by the mass flow controller (M). Once the samples were introduced to the sampling system,  $\text{HONO}(\text{g})$  and  $\text{NO}_2^-(\text{p})$  were

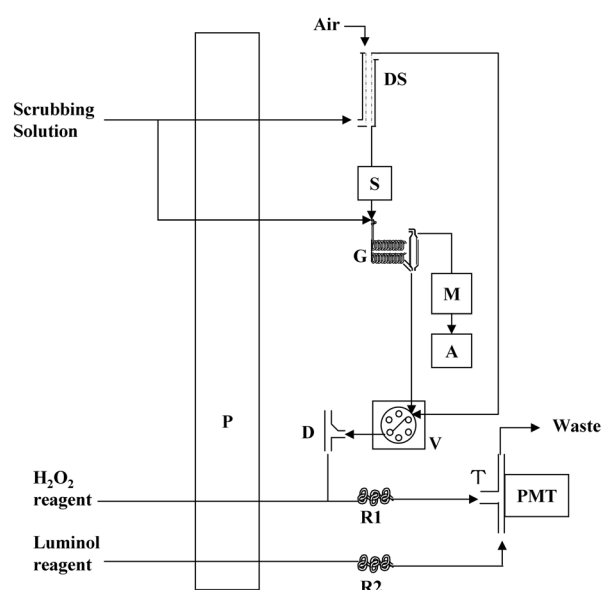


**Figure 1.** A schematic diagram of the measurement system: A, vacuum air pump; D, glass debubbler; DS, diffusion scrubber; G, glass coil; M, mass flow controller; P, peristaltic pump; R1, R2, knotted reactor; S, steam generator and particle collection section; T, quartz tee; V, six-port valve.

collected in two separate devices; the former in diffusion scrubber (DS) and the latter in steam reactor (S). The DS was composed of a pair of concentric tubes (60 cm in length). The inner tube was a microporous polypropylene membrane (5.5 mm i.d., 1.55 mm thickness, 70% surface porosity,  $0.20 \mu\text{m}$  mean pore size; Accurel PP V8/2 HF, Membrana, Germany) and the outer was a glass tube (9 mm i.d., 1.2 mm thickness). The scrubbing solution was pumped continuously at a flow rate of  $0.63 \text{ mL min}^{-1}$  between the membrane and the glass tubing. As the samples passed through the DS,  $\text{HONO}(\text{g})$  was absorbed on the surface of the microporous membrane wall. The collected  $\text{HONO}(\text{g})$  was then dissolved in the scrubbing solution of the first channel. Since  $\text{NO}_2^-(\text{p})$  was not adsorbed on the DS surface, it passed down to the end of the DS, grew in size in the steam reactor, and then was dissolved into the scrubbing solution in the 10-turn glass coil (G). All solution used in this system are pumped through Teflon tubing (Cole-Parmer PTFE tubing) by a multichannel peristaltic pump (P).

In this study, a home-built particle collection system (PCS) was used for the  $\text{NO}_2^-(\text{p})$  collection (see Fig. 2). In principle, the system was identical to the well-established PCS, found in the previous studies.<sup>20,29,30</sup> The hot steam was generated by passing deionized water (DW) through a heating apparatus. The steam was injected into the steam reactor and then mixed with particles. This process promoted the particle size large enough to be collected by both condensation and inertial impaction. The steam reactor was constructed in a cylindrical shape with approximately  $100 \text{ cm}^3$  of inner volume. To maintain the supersaturation condition ( $\sim 300\%$ ), the reactor was cooled at  $25\text{--}30 \text{ }^\circ\text{C}$  by a water circulation system enclosing it. The accelerating nozzle was placed at the outlet of the reactor so that the effluent from the

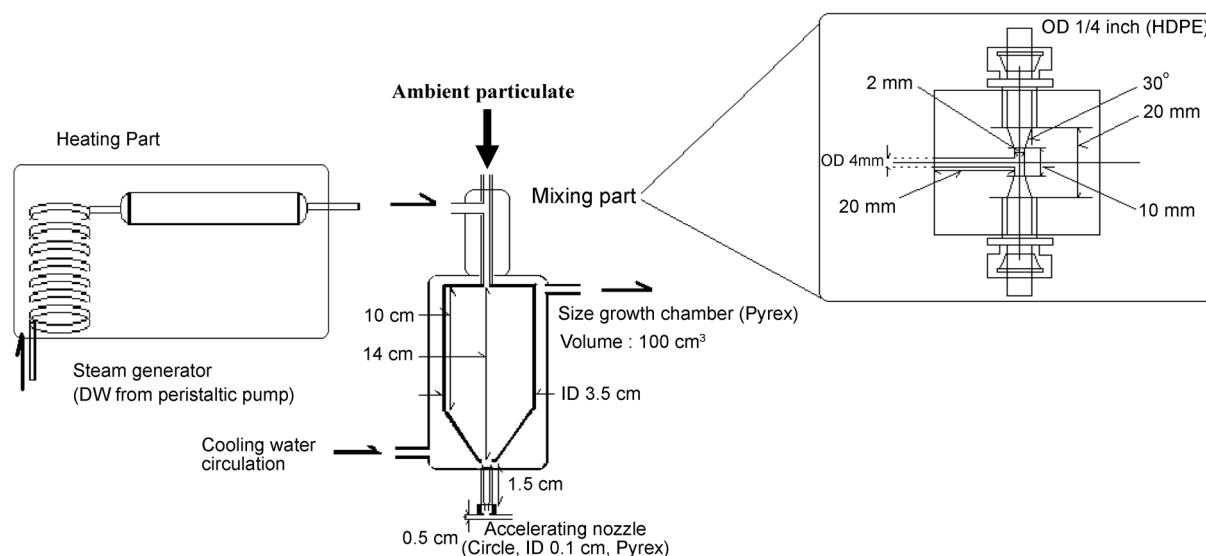


**Figure 2.** A schematic diagram of the particle collection section.

reactor was strongly impacted and efficiently collected into DW flowing through a coil sampler. The PCS was optimized for the flow rates of steam and DW flowing through the coil. The optimal rates for both parameters were identical and found to be over  $\sim 0.17 \text{ mL min}^{-1}$ .

**Automated sample injection system.** After collected by their respective sampling apparatuses, the gas- and particle-phase samples were supplied to the automated sample injection system. The injection system delivered the samples to the analytical system. The injection apparatus was composed of two devices: a fluid processor and a debubbler (D). The fluid processor was an automated six-port valve (V) with a time controller (AT3000, Futecs, Korea). The two ports of six-port valve were connected to the gas- and particle-phase sample lines. The valve rotated automatically to two positions to load either gas- or particle-phase samples every two-minute interval in an alternating manner. Therefore, the time resolution of the whole system was 4 minutes. Valve switching timing was regulated by the time controller. A debubbler was used to remove bubbles in the samples after passing through the fluid processor.

**Analytical system.** The analytical method was based on peroxyxynitrite-induced luminol chemiluminescence, involving two key reactions.<sup>31,32</sup> In an acidic medium, the dissolved nitrite in the samples reacts with hydrogen peroxide to produce peroxyxynitrous acid (HOONO). And then, in a strong alkaline medium, the dissociated peroxyxynitrite ( $\text{ONOO}^-$ ) reacts with luminol to emit chemiluminescent light (CL). By detecting the chemiluminescence using a photomultiplier tube (PMT), the concentrations of dissolved nitrite samples are quantified. For the first reaction, in a reaction coil (R1), the sample flow, containing nitrite ion in 0.1 M phosphate buffer solution, was mixed with the reagent stream consisting of 0.22 mM  $\text{H}_2\text{O}_2$  and 3 mM EDTA in 0.26 M  $\text{H}_2\text{SO}_4$  medium. For the second reaction, in another reaction coil (R2), the chemiluminescent solution containing 1 mM luminol was mixed with 3 mM EDTA in 0.75 M NaOH. The

two streams were merged in a reaction cell in front of the PMT (Hamamatsu, H5784-01) and the CL was measured. The wavelengths of the emitted CL ranged between about 350 and 650 nm.<sup>31</sup> The peak height in the CL spectrum represented the signal of the analytical system in a unit of mV. The cell was a T-shaped quartz tube (2 mm i.d.) with two inlets for the luminol and sample streams and an outlet for waste. Two identical reaction coils (PTFE, 0.6 mm i.d.  $\times$  30 cm length) were utilized for both reactions. Since light other than the CL might penetrate into the reaction cell and interfere with the CL, the reaction cell was ensured to be sealed off completely to avoid such an artifact. The housing of the cell was not commercially available and thus it was home-built with stainless steel. If two detectors, one for HONO(g) and the other for  $\text{NO}_2^-$ (p), are employed, the integration time of the whole system can be reduced from 4 to 2 minutes. Thus, it is possible to monitor these two species in more continuous manner.

**Reagents.** All reagent solutions were prepared with water purified by Milli-Q water system with resistivity  $\geq 18.2 \text{ M}\Omega$ . The scrubbing solution was 0.1 M  $\text{Na}_2\text{HPO}_4$  (Sigma Chemical), adjusted to pH 7.0 with NaOH (Sigma Chemical). The luminol reagent solution was made up of 3 mM luminol (Sigma Chemical) and 3 mM disodium dihydrogen ethylene diamine tetraacetate dehydrate ( $\text{EDTA-2Na}$ , Sigma Chemical) in 0.75 M of NaOH medium. The  $\text{H}_2\text{O}_2$  reagent was prepared with 0.22 mM  $\text{H}_2\text{O}_2$  (Sigma Chemical) and 3 mM  $\text{EDTA-2Na}$  in 0.26 M  $\text{H}_2\text{SO}_4$  (Sigma Chemical) medium. The nitrite ( $\text{NO}_2^-$ ) standard solution was made with sodium nitrite ( $\text{NaNO}_2$ , Sigma Chemical) and was diluted with 0.1 M  $\text{Na}_2\text{HPO}_4$ .

## Experimental Results

**Collection efficiency of HONO(g).** To determine the collection efficiency of HONO(g) by the DS with respect to flow rates of air samples, a number of laboratory experi-

ments were conducted. The air samples were collected by using two identical DS connected in series so that the second DS collect the effluent from the first DS. The collection efficiency ( $\beta$ ) was then determined from the ratio of the HONO(g) collected by the two DS, using the following equation.<sup>33</sup>

$$\beta = (1 - C_2/C_1) \times 100\% \quad (1)$$

, where  $C_1$  and  $C_2$  denoted the concentration of HONO(g) collected by the first and the second DS, respectively. As shown in Figure 3,  $\beta$  increased from 86% to 98% as the air flow rate decreased from 1.5 to 0.5 L min<sup>-1</sup>. On the other hand, the collection efficiency of NO<sub>2</sub><sup>-</sup>(p) was observed to be elevated with increasing air flow rate. Therefore, it was necessary to compromise the collection efficiencies of HONO(g) and NO<sub>2</sub><sup>-</sup>(p) in reasonable limits. As a result, the optimal air flow rate was chosen to 1 L min<sup>-1</sup> at which approximately 91% of HONO(g) was collected.

**Particle transmission and collection efficiencies.** To find out the efficiency with which particles pass through the DS (*i.e.*, particle transmittance efficiency (PTE)) without absorption to the DS surface, experiments were conducted in a wide range of aerosol sizes. By employing an aerosizer (API Inc., Model Mach II), the PTE was determined as a number concentration ratio ( $N_{\text{out}}/N_{\text{in}}$ ) multiplied by 100, where  $N_{\text{in}}$  and  $N_{\text{out}}$  represented the particle number concentrations measured at the inlet and at the outlet of the DS, respectively. Figure 4 illustrates the resulting PTE variations with particle size from 0.2 to 3.2  $\mu\text{m}$ . Virtually 100% of particles with aerodynamic diameters ( $D_p$ ) larger than 1  $\mu\text{m}$  were transmitted through the DS. Even the submicron particles ( $0.2 < D_p < 1 \mu\text{m}$ ) penetrated through the DS with the PTEs greater than 97%. In addition, particle collection efficiency (PCE) in the steam reactor was measured over the  $D_p$  range between 0.2 and 3.2  $\mu\text{m}$ . Particles with  $D_p$  larger than 0.5  $\mu\text{m}$  were accumulated with near 100% of PCEs. The PCEs of smaller particles ( $0.2 < D_p < 0.5 \mu\text{m}$ ) were reduced with decreasing  $D_p$ , nonetheless still over 90%.<sup>34</sup>

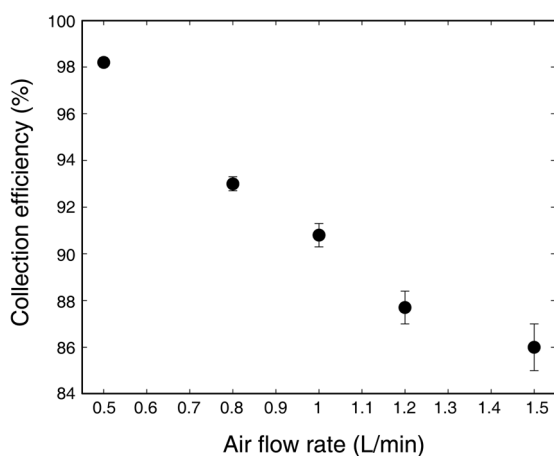


**Figure 3.** Experimental collection efficiency of HONO(g) as a function of gas flow rate. The filled circles and error bars denote the mean values ( $M$ ) and one standard deviation from the means ( $\pm 1 \sigma$ ), respectively.

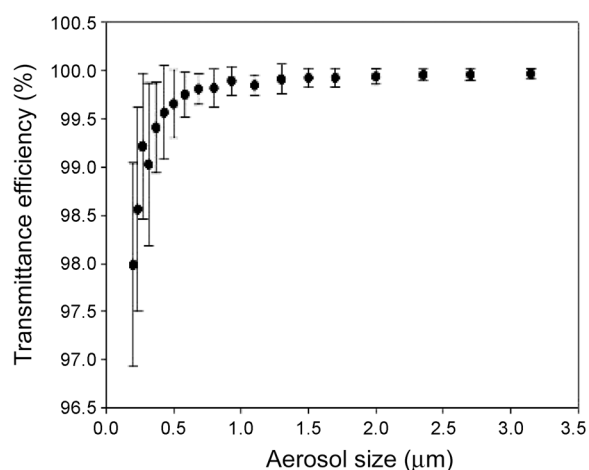


**Figure 4.** Particle transmittance efficiency as a function of particle size.

**Optimization of analytical system.** To attain the best chemiluminescence signals, the analytical system was optimized by adjusting PMT voltage and by modifying chemical conditions of luminol and H<sub>2</sub>O<sub>2</sub> reagents. Details on optimization studies follow where the limit of detection (LOD) refers to the detected signal reported as mixing ratio of gaseous nitrous acid.

**PMT voltage:** In this study, the voltage of PMT was found to be one of the most important parameters controlling the LOD of the analytical system. As seen in Figure 5a, the LOD of the system was exponentially decreased approximately from 290 to 100 pptv by about a factor of three with increasing voltages from 650 to 1200 mV. Clearly, at the voltages  $\geq 900$  mV, the LOD was not improved but remained almost constant. Therefore, 900 mV was determined as the optimal PMT voltage.

**Luminol reagent:** Optimization procedures regarding the luminol reagent focused on three key parameters, *i.e.*, pH, luminol concentration, and flow rate of the reagent. In acidic medium, no chemiluminescent light (CL) signals were detected, accentuating the significance of pH in the luminol reagent solution. At 1 mM of luminol and 0.42 mL min<sup>-1</sup> of flow rate, the CL intensity varied parabolically with the pH (Fig. 5b). It was elevated from about 1.1 to 1.4 mV with the increasing pH from 13.4 to 13.6 and then decreased in the pH range between 13.6 and 13.8. This indicates that the CL signal was quite sensitive to pH, varying by about 30% with 0.4 pH change. The optimal pH (*i.e.*, 13.6) was chosen at which the maximum signal was observed.

The sensitivity of detection limit to luminol concentration was also examined at pH 13.6 and 0.42 mL min<sup>-1</sup> of flow rate. The LOD varied with the luminol concentration in a V-shape (Fig. 5c). About 5% of the LOD was improved with the increasing concentration from 0.4 to 1 mM by a factor of 2.5. In contrast, the LOD was deteriorated by 5% with the increasing concentration from 1 to 1.4 mM. Although not shown in Figure 3c, additional experiments were conducted in the broader concentration range between 0.2 and 4 mM. Nonetheless, the best LOD was observed to be approxi-

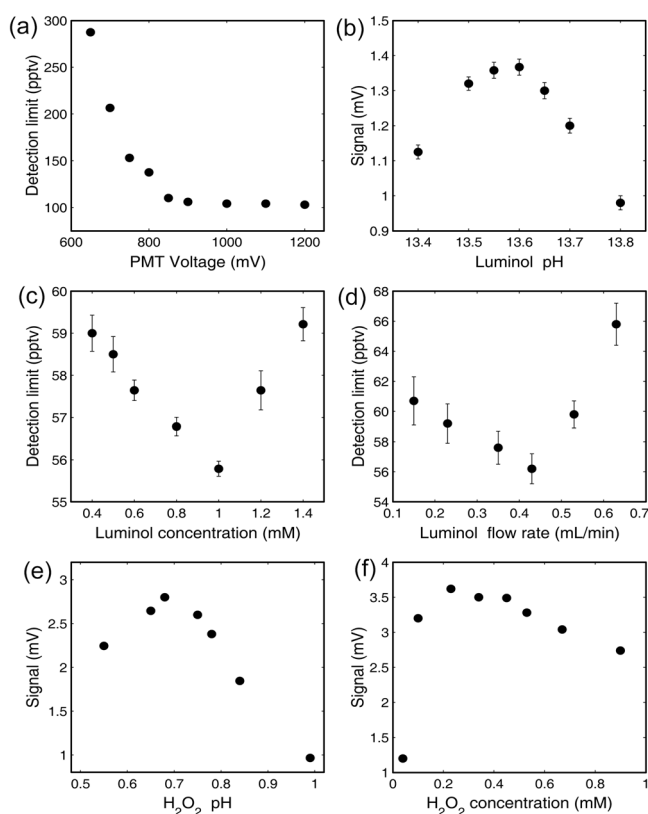


**Figure 5.** Optimization results of 6 parameters. (a) Detection limit at different PMT voltages. The detection limit refers to a detected signal that was converted to volume mixing ratio of HONO(g). (b) Signal intensity as a function of luminol reagent pH. (c) Detection limit dependence of luminol concentration. (d) Detection limit as a function of luminol reagent flow rate. (e) Signal intensity variation with the H<sub>2</sub>O<sub>2</sub> reagent pH. (f) Signal intensity change with H<sub>2</sub>O<sub>2</sub> concentration. Refer to Figure 2 for the meaning of filled circles and error bars.

mately 56 pptv at 1 mM of luminol concentration.

At pH 13.6 and 1 mM of luminol concentration, sensitivity of the LOD to the luminol flow rate was investigated. The LOD variation was V-shaped with the flow rate (Fig. 5d). However, the flow rate appeared to be a little more sensitive parameter than the luminol concentration. The LOD was changed from 56 to 66 pptv by about 15%, depending on luminol reagent flow rate ranging between 0.15 and 0.65 mL min<sup>-1</sup>. The best detection limit was found at the flow rate of 0.42 mL min<sup>-1</sup>.

**H<sub>2</sub>O<sub>2</sub> reagent:** A strong acidic medium was a critical requirement for the formation of pernitrous acid *via* the reaction between NO<sub>2</sub><sup>-</sup> and H<sub>2</sub>O<sub>2</sub>. Although experiments were carried out over the wider pH range, the results were presented in the pH range between 0.5 and 1.0 (Fig. 5e). The strongest CL intensity was observed at the pH ~ 0.7 which was chosen as the optimum pH in this study.

The impact of H<sub>2</sub>O<sub>2</sub> concentration on the CL intensity was also examined in the range between 0.04 and 0.88 mM (Fig. 5f). The CL intensity increased drastically from 0.04 up to 0.22 mM of H<sub>2</sub>O<sub>2</sub> whereas it tended to decrease gradually at higher concentrations. 0.22 mM of H<sub>2</sub>O<sub>2</sub> was adopted as the

optimum value in this work.

To avoid potential interferences of metal cations (*i.e.*, catalysis of the CL reaction between H<sub>2</sub>O<sub>2</sub> and luminol), EDTA-2Na has been frequently employed in this type of CL technique.<sup>31,32</sup> As reported in the previous studies cited, 3 mM EDTA-2Na was found to be the optimal.

**Calibration curve and detection limit.** Under the optimal conditions obtained from the above optimization experiments (summarized in Table 1), calibrations were conducted in the range of standard nitrite solutions between 0 and 50 mM. The resulting calibration curve was linear with a 0.9988 of R<sup>2</sup> value and was expressed as  $y = 1.98 \times 10^{-4} x - 3.19 \times 10^{-3}$ , where  $y$  and  $x$  denote the signal and nitrite concentration, respectively. Based on a signal to noise ratio of 3, the detection limit of the whole system was determined to be 13 pptv.

The performance of our instrument was intercompared with those of other systems (see Table 2). In the previous studies, the ion chromatography was utilized as a detection method and the samples were integrated to pre-concentration columns in order to determine low concentrations of dissolved NO<sub>2</sub><sup>-</sup> ions. In this study, on the other hand, a flow injection system with a chemiluminescence technique was used for the faster sample delivery and more sensitive detection. Consequently, this study could attain the shorter time resolution and the similar or better detection limit, compared to the previous studies.

**Interferences.** In alkaline solution, once dissolved, PAN and NO<sub>2</sub> can yield nitrite ions by reaction with OH<sup>-</sup>.<sup>15</sup> Therefore, if alkaline-coatings or alkaline scrubbing solutions were utilized in the DS and the steam chamber, the positive artifacts can be significant.<sup>2,26,27,35,36</sup> To avoid these positive interferences, for a scrubbing solution, we used 0.1 M Na<sub>2</sub>HPO<sub>4</sub> solution, adjusted to pH 7.0 with NaOH.

In the two previous studies where the DS was used,<sup>15,16</sup> the interferences in the DS were found to be negligible. Vecera and Dasgupta (1991a) reported only 0.022% of positive interference from NO<sub>2</sub>. Kanda and Taira (1990) found no major positive artifacts (1.9% from PAN and 0.4% from NO<sub>2</sub>). Wet effluent diffusion denuders (WEDD) have been most widely used for HONO(g) collection and a DS is essentially a type of WEDD.<sup>22</sup> In the WEDD without alkaline coatings, interferences from NO, NO<sub>2</sub>, and PAN were reported to be less than 0.1%, 0.1%, and 0.52%, respectively

**Table 1.** Standard conditions used for optimization of the analytical system

Parameters	Values
PMT voltage	900 mV
Luminol reagent pH	13.6
Luminol reagent concentration	1 mM
Luminol reagent flow rate	0.42 mL min <sup>-1</sup>
H <sub>2</sub> O <sub>2</sub> reagent pH	0.7
H <sub>2</sub> O <sub>2</sub> reagent concentration	0.22 mM
EDTA-2Na concentration	3 mM
Nitrite concentration in 0.1 M Na <sub>2</sub> HPO <sub>4</sub>	25 ppbv

**Table 2.** The results of intercomparisons between simultaneous measurements systems of HONO(g) and NO<sub>2</sub><sup>-</sup>(p)

	Methods	Limits of Detection	Frequencies
This study	Diffusion Scrubber / Steam chamber / Luminol chemiluminescence	HONO(g) and NO <sub>2</sub> <sup>-</sup> (p); 13 pptv	4 min
Fisseha <i>et al.</i> , 2006	Wet effluent diffusion denuder / Steam chamber / Ion chromatography	HONO(g) and NO <sub>2</sub> <sup>-</sup> (p); 1-20 ng/m <sup>3</sup>	2 hour
Acker <i>et al.</i> , 2005	Wet effluent diffusion denuder / Steam chamber / Ion chromatography	HONO(g) and NO <sub>2</sub> <sup>-</sup> (p); 10 ng/m <sup>3</sup>	30 min ~ 1 hour
Trebs <i>et al.</i> , 2004	Wet annular denuder / Steam chamber / Ion chromatography	HONO(g); 12 pptv, NO <sub>2</sub> <sup>-</sup> (p); 9 pptv	20 ~ 60 min
Neftel <i>et al.</i> , 1996	Wet effluent diffusion denuder / Steam chamber / Ion chromatography	HONO(g); 100 ng/m <sup>3</sup> , NO <sub>2</sub> <sup>-</sup> (p); 40 ng/m <sup>3</sup>	~15 min
Simon <i>et al.</i> , 1995	Parallel plate diffusion denuder / Steam chamber / Ion chromatography	NO <sub>2</sub> <sup>-</sup> (p); 0.6 ng/m <sup>3</sup>	16 min
Li <i>et al.</i> , 1994	Coating denuders / filter pack / Ion chromatography	NO <sub>2</sub> <sup>-</sup> ; 1.7 pptv	24 hour
Zellweger <i>et al.</i> , 1993	Wet effluent diffusion denuder / Steam chamber / Ion chromatography	HONO(g) and NO <sub>2</sub> <sup>-</sup> (p); a few ng/m <sup>3</sup>	~60 min

(Table 2 in Neftel *et al.*, 1996). Zellweger *et al.* (1999) found 0.1% interference for NO<sub>2</sub> up to 318 ppb. Artifacts from NO<sub>2</sub> increased from 0.003 to 0.01% with increasing pH from 4 to 8, respectively. They also found the interference from PAN to be  $1.3 \pm 0.3\%$ .<sup>37</sup> Even in alkaline-coated WEDD, Spindler (2003) found the interference to be 0.56% of NO<sub>2</sub>.

Furthermore, in the DS used in this study, the residence time of an air sample was very short (3.4 s) and the scrubbing solution residence time was also short (24 s). Even if the interfering reaction took place, there would not be sufficient time for the gas to contact with the wetted DS surface. Therefore, this short residence time will minimize interferences by NO<sub>2</sub> and SO<sub>2</sub>, as other studies indicated.<sup>26,38</sup>

Since the development of simultaneous gas/particle collection and analysis principle by Simon and Dasgupta (1995), a number of studies, including this study, have made use of the similar instrumental design to concurrently measure HONO(g) and NO<sub>2</sub><sup>-</sup>(p).<sup>21,24-27,36</sup> In these studies, interferences from gases such as NO, NO<sub>2</sub>, PAN, and SO<sub>2</sub> in the particle collection system were investigated. Simon and Dasgupta (1995) examined the interferences from NO (0-250 ppbv) and NO<sub>2</sub> (0-80 ppbv) and concluded that artifacts by NO and NO<sub>2</sub> were 0.11% and 0.02%, respectively. Neftel *et al.* (1996) reported that in the steam chamber, interferences from NO, NO<sub>2</sub>, and PAN were < 0.1%, 0.25%, and 0.4%, respectively. Zellweger *et al.* (1999) found that the artifact by NO<sub>2</sub> was highly variable between 0.2 and 1% of the NO<sub>2</sub> inflowing from the denuder.

For the liquid-phase interference in the analytical system, the previous studies using the peroxyxynitrite-induced luminol chemiluminescence described potential interferences from various dissolved ions in detail.<sup>31,32</sup> The results demonstrated that interferences were not significant with an exception of high concentrations of hypochlorite.

Since we utilized the collection systems (*i.e.*, DS and steam chamber) similar to those in the literature with a neutral scrubbing solution and pure water for the steam generation, the artifacts from NO<sub>2</sub> and PAN are expected to

be in the ranges reported in the previous studies.

**Intercomparison between luminol chemiluminescence and IC technique.** To verify the analytical system for nitrite, the luminol chemiluminescence method was inter-compared to IC method, one of the well-established methods. Identical standard nitrite solutions with various concentrations were prepared and analyzed simultaneously by both methods. The standard solutions concentrations ranged between 0.0435 and 0.435 μM. Experiments using IC method were carried out with an eluent solution (3.5 mM Na<sub>2</sub>CO<sub>3</sub> + 1 mM NaHCO<sub>3</sub>) and an analysis column (Dionex – AS 14A; 250 mm in length and 4 mm i.d.). The flow rate of the eluent was 1.2 mL min<sup>-1</sup>. A linear regression analysis gave a correlation coefficient of 0.9990, a slope of 0.9994, and a y-intercept of  $1.214 \times 10^{-4}$  (Fig. 6). This result clearly indicates that the method used in this study is appropriate for monitoring total HONO in the atmosphere.

#### Field measurements of HONO(g) and NO<sub>2</sub><sup>-</sup>(p)

Using this new instrument, field measurements of HONO (g) and NO<sub>2</sub><sup>-</sup>(p) were made in springtime from March 16 to April 17, 2004 at GIST (Gwangju Institute of Science and Technology), Gwangju, South Korea. Gwangju is one of major cities in South Korea with a population of about 1.4 million. GIST is located in the northern part of the city substantially away from the downtown pollution sources (35°10'N and 126°50'E). The samples of gas- and particulate-phase HONO were collected on the roof of the mobile trailer (6 m height above ground) at GIST. In addition, other trace gases and meteorological parameters were simultaneously observed.

**Diurnal cycles of gaseous nitrous acid, particulate nitrite, and total HONO.** Figure 7a-7d show diurnal variations of gaseous nitrous acid (HONO(g)), nitrite (NO<sub>2</sub><sup>-</sup>(p)), total HONO (HONO(g) + NO<sub>2</sub><sup>-</sup>(p)), and the ratio of NO<sub>2</sub><sup>-</sup>(p) to HONO(g), respectively. In these figures, only hourly averaged data, collected from April 5 to 17, 2004, are

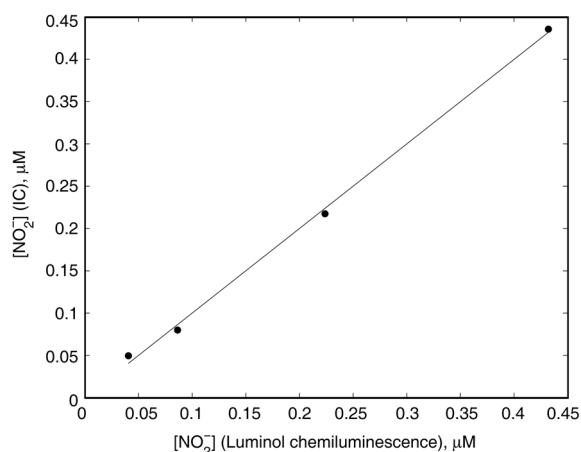


**Figure 6.** Intercomparison between luminol chemiluminescence and IC technique.

presented. The filled circles and error bars represent hourly means ( $M$ ) and one standard deviations ( $\sigma$ ), respectively. In Figure 7a, solar radiation intensities are also displayed as three solid lines:  $M + \sigma$ ,  $M$ , and  $M - \sigma$  from the top to the bottom, respectively.

In the earlier observational<sup>17,27</sup> and modeling studies,<sup>6,39,40</sup> concentrations of HONO(g) were found to increase due to the heterogeneous chemistry after sunset, to reach the daily maximum level just before sunrise, and to continuously decrease after sunrise due to its photolysis. By comparing the daily variation of HONO(g) with that of solar radiation intensity, the daily maximum HONO(g) was found to coincided with sunrise at 5 A.M.. The diurnal trend was similar to those found in the earlier studies (Fig. 7a). The HONO(g) levels were also within the range observed or predicted in the previous studies. On the basis of the mean values, the nighttime maximum and the daytime minimum were approximately 0.864 ppbv at 5 A.M. and 0.159 ppbv at 2 P.M., respectively. This indicated that HONO(g) concentration could fluctuate in a day on average by a factor of 5.4.

In contrast to HONO(g), the diurnal variation of particulate nitrite was not pronounced and did not show the distinctive maximum and minimum (Fig. 7b). A broad peak (0.206-0.242 ppbv) was found between 8 A.M. and 11 A.M. with the maximum (0.242 ppbv) at 11 P.M.. An extended bottom (0.167-0.173 ppbv) was observed between 1 P.M. and 6 P.M. with the minimum (0.167 ppbv) at 4 P.M..

A correlation between HONO(g) and  $\text{NO}_2^-(\text{p})$  was investigated only in a small number of studies<sup>20,24</sup> in which the two species were measured concurrently. Simon and Dasgupta (1995) observed a strong positive correlation, however the findings of Fisseha *et al.* (2006) were mixed. For instance, for the data obtained in March, 2003, the diurnal variations of HONO(g) and  $\text{NO}_2^-(\text{p})$  were in good agreement; the maxima and the minima of the two species occurred simultaneously and distinctively (see Figure 6 of Fisseha *et al.*, 2006). For the data collected in August and September, 2002, on the other hand, that was not the case. Our result showed that the correlation was positive but weak with a

coefficient of 0.27. It is not certain what process was responsible for this weak correlation. Clearly, further research is needed.

As seen in Figure 7a with 7b, it is obvious that HONO(g) levels dominated those of  $\text{NO}_2^-(\text{p})$ . For the data collected during the entire experiments, the mean value of HONO(g) (0.479 ppbv) was higher by about a factor of 2.4 than that of  $\text{NO}_2^-(\text{p})$  (0.198 ppbv). As a result, the daily variation pattern of the total HONO was almost identical to that of HONO(g), reflecting the much higher concentration levels of HONO(g) than  $\text{NO}_2^-(\text{p})$  (Fig. 7c). Similarly, the maximum and the minimum of total HONO were found to be about 1.05 ppbv at 5 A.M. and 0.33 ppbv at 2 P.M. with a diurnal fluctuation by about a factor of three.

In order to investigate the diurnal variations in HONO partitioning between gas- and aerosol-phase, the ratios of  $\text{NO}_2^-(\text{p})$  to HONO(g) were displayed in Figure 7d. Between 11 P.M. and 7 A.M., the ratios were lower than 0.5, however, between 1 P.M. and 5 P.M., the ratios were higher than 1.0.

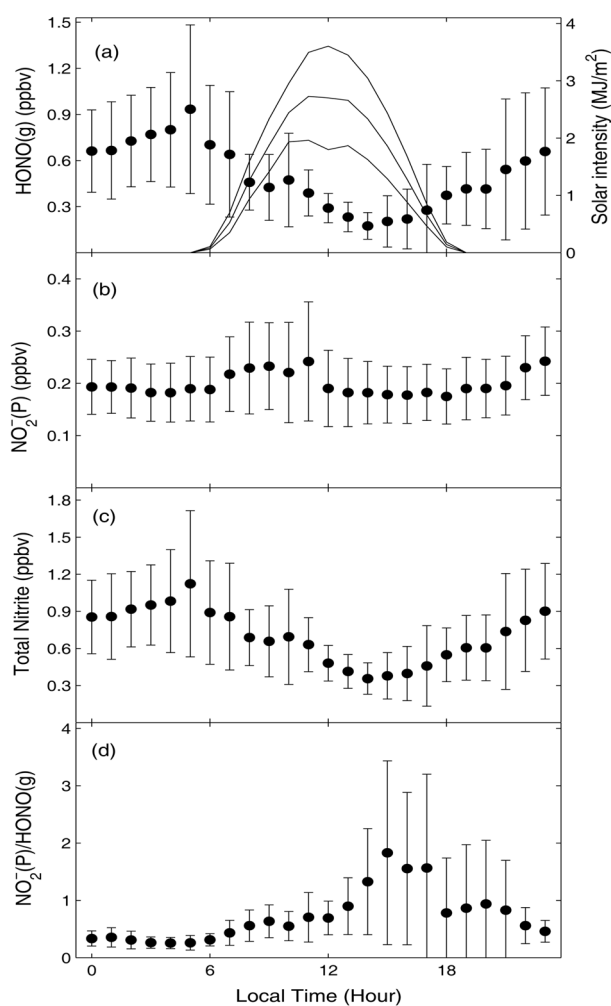


**Figure 7.** Diurnal variations of (a) HONO(g), (b) particulate nitrite ( $\text{NO}_2^-(\text{p})$ ), (c) total HONO (HONO(g) +  $\text{NO}_2^-(\text{p})$ ), and (d)  $[\text{NO}_2^-(\text{p})]/[\text{HONO}(\text{g})]$  ratio observed for April 2-17, 2004. Refer to Figure 2 for the meaning of filled circles and error. In Figure 6(a), three solid lines represents solar radiation intensity,  $M + \sigma$ ,  $M$ , and  $M - \sigma$  from the top to the bottom, respectively.

The daily maximum (1.76) was found at 3 P.M., while the daily minimum (0.26) at 3 A.M.. During night HONO(g) was more abundant than NO<sub>2</sub><sup>-</sup>(p), whereas during day the latter was comparable to or sometimes exceeded the former. These results indicate that particularly in the daytime, a significant fraction of the total HONO was present as the aerosol form. Thus, this emphasizes the necessity of concurrent measurements of particle- and gas-phase HONO, particularly during daytime.

### Conclusion

A new instrument for simultaneous measurements of gas- and particle-phase HONO was developed, based upon the diffusion scrubber/steam chamber/luminol chemiluminescence. To separately collect HONO(g) and NO<sub>2</sub><sup>-</sup>(p), the DS and home-built particle growth chamber were utilized, respectively. The collection efficiency of HONO(g) by the DS was estimated to be 90.8 ± 0.5%. For large particles (D<sub>p</sub> > 1 μm), the particle transmittance efficiencies (PTEs) were almost 100%, and for submicron particles (0.2 < D<sub>p</sub> < 1 μm), the PTEs were higher than 97%. Particles (D<sub>p</sub> > 0.5 μm) were collected with near 100% of particle collection efficiencies (PCEs). The PCEs of smaller particles (0.2 < D<sub>p</sub> < 0.5 μm) were reduced with decreasing D<sub>p</sub>, nonetheless still over 90%. The optimal conditions found were 900 mV of the PMT Voltage, 13.6 of luminol reagent pH, 1 mM of luminol concentration, 0.42 mL min<sup>-1</sup> of luminol reagent flow rate, 0.7 of H<sub>2</sub>O<sub>2</sub> reagent pH, 0.22 mM of H<sub>2</sub>O<sub>2</sub> concentration, and 3 mM of EDTA-2Na. Under these conditions, the detection limit of the instrument was estimated to be 13 pptv with 4 minutes of time resolution. This new technique was applied to field measurements of HONO(g) and NO<sub>2</sub><sup>-</sup>(p) made in springtime from March 16 to April 17, 2004 in Gwangju, South Korea. When HONO(g), NO<sub>2</sub><sup>-</sup>(p), and total nitrite were compared, a substantial portion of the total nitrite was found to exist as an aerosol form, particularly during daytime.

**Acknowledgments.** This work was supported by the Korea Research Foundation Grant funded by Korea Government (MOEHRD, Basic Research Promotion Fund) (KRF-2005-075-c00037). This work was also supported in part by the Korea Science and Engineering Foundation (KOSEF) through the Advanced Environmental Monitoring Research Center (ADEMRC) at Gwangju Institute of Science and Technology and the Brain Korea 21 Project, Ministry of Education and Human Resources Development (MOE), South Korea.

### References

- Thompson, A. M. *Science* **1992**, 256, 1157.
- Lammel, G.; Cape, J. *Chemical Society Review* **1996**, 25, 361.
- Alicke, B.; Platt, U.; Stutz, J. *Journal of Geophysical Research* **2002**, 107, 8196.
- Alicke, B.; Geyer, A.; Hofzumahaus, A.; Holland, F.; Konrad, S.; Patz, H.-W.; Schafer, J.; Stutz, J.; Volz-Thomas, A.; Platt, U. *Journal of Geophysical Research* **2003**, 108, 8247.
- Harrison, R. M.; Peak, J. D.; Collins, G. M. *Journal of Geophysical Research* **1996**, 101, 14429.
- Kotamarthi, V. R.; Gaffney, J. S.; Marley, N. A.; Doskey, P. V. *Atmospheric Environment* **2001**, 35, 4489.
- Perner, D.; Platt, U. *Geophysical Research Letter* **1979**, 6, 917.
- Platt, U.; Perner, D.; Harris, G. W.; Winer, A. M.; Pitts, Jr., J. N. *Geophysical Research Letter* **1980**, 7, 89.
- Clemmshaw, K. C. *Critical Reviews in Environmental Sciences and Technology* **2004**, 34, 1.
- Parrish, D. D.; Fehsenfeld, F. C. *Atmospheric Environment* **2000**, 34, 1921.
- Rodgers, M. O.; Davis, D. D. *Environmental Science and Technology* **1989**, 23, 1106.
- Ferm, M.; Sjodin, A. *Atmospheric Environment* **1985**, 19, 979.
- Appel, B. R.; Winer, A. M.; Tokiwa, Y.; Biermann, H. W. *Atmospheric Environment* **1990**, 24(A), 611.
- Febbo, A.; Perrino, C.; Cortiello, M. *Atmospheric Environment* **1993**, 27(A), 1721.
- Kanda, Y.; Taira, M. *Analytical Chemistry* **1990**, 62, 2084.
- Vecera, Z.; Dasgupta, P. K. *Environmental Science and Technology* **1991a**, 25, 255.
- Zhou, X.; Qiao, H.; Deng, G.; Civerolo, K. *Environmental Science and Technology* **1999**, 33, 3672.
- Vecera, Z.; Dasgupta, P. K. *Analytical Chemistry* **1991b**, 63, 2210.
- Simon, P. K.; Dasgupta, P. K.; Vecera, Z. *Analytical Chemistry* **1991**, 63, 1237.
- Simon, P. K.; Dasgupta, P. K. *Analytical Chemistry* **1995**, 67, 71.
- Zellweger, C.; Ammann, M.; Hofer, P.; Baltensperger, U. *Atmospheric Environment* **1999**, 33, 1131.
- Genfa, Z.; Slanina, S.; Boring, B. C.; Jongejan, P. A. C.; Dasgupta, P. K. *Atmospheric Environment* **2003**, 37, 1351.
- Dasgupta, P. K. *Wilson and Wilson's Comprehensive Analytical Chemistry Series*; Elsevier: 2002; Vol. 37, p 97.
- Fisseha, R.; Dormmen, J.; Gutzwiller, L.; Weingartner, E.; Gysel, M.; Emmenegger, C.; Kalberer, M.; Baltensperger, U. *Atmospheric Chemistry and Physics* **2006**, 6, 1895.
- Acker, K.; Moller, D.; Auel, R.; Wieprecht, W.; Kalaß, D. *Atmospheric Environment* **2005**, 74, 507.
- Trebs, I.; Meixner, F. X.; Slanina, J.; Otjes, R.; Jongejan, P.; Andreae, M. O. *Atmospheric Chemistry and Physics* **2004**, 4, 967.
- Nefel, A.; Blatter, A.; Hesterberg, R.; Steffebach, T. *Atmospheric Environment* **1996**, 30, 3017.
- Li, S. *Journal of Geophysical Research* **1994**, 99, 25469.
- Khlystov, A.; Wyers, G.; Slanina, J. *Atmospheric Environment* **1995**, 29, 2229.
- Webber, R. J.; Orsini, D.; Daun, Y.; Lee, Y.-N.; Klotz, P. J.; Brechtel, F. *Aerosol Science and Technology* **2001**, 35, 718.
- Mikuska, P.; Vecera, Z.; Zdrahal, Z. *Analytica Chimica Acta* **1995**, 316, 261.
- Mikuska, P.; Vecera, Z. *Analytica Chimica Acta* **2003**, 495, 225.
- Dasgupta, P. K.; Dong, S.; Hwang, H.; Yang, H.-C.; Genfa, Z. *Atmospheric Environment* **1988**, 22, 949.
- Hong, S. B.; Kim, D. S.; Ryu, S. Y.; Kim, Y. J.; Lee, J. H. *Atmospheric Research* **2008**, 89, 62.
- Spindler, G.; Hesper, J.; Bruggemann, E.; Dubois, R.; Muller, Th.; Herrmann, H. *Atmospheric Environment* **2003**, 37, 2643.
- Loflund, M.; Kasper-Giebl, A.; Tschewenka, W.; Schmid, M.; Giebl, H.; Hitznerberger, R.; Reischl, G.; Puxbaum, H. *Atmospheric Environment* **2001**, 35, 2861.
- Takenaka, N.; Terada, H.; Oro, Y.; Hiroi, M.; Yoshikawa, H.; Okitsu, K.; Bandow, H. *Analyst* **2004**, 129, 1130.
- Acker, K.; Spindler, G.; Bruggemann, E. *Atmospheric Environment* **2004**, 38, 6497.
- Vogel, B.; Vogel, H.; Kleffmann, J.; Kurtenbach, R. *Atmospheric Environment* **2003**, 37, 2957.
- Aumont, B.; Chervier, F.; Lavel, S. *Atmospheric Environment* **2003**, 37, 487.